Theoretical Transport Analysis of Density limit with Radial Electric Field in Helical Plasmas

S. Toda 1) and K. Itoh 1)

1) National Institute for Fusion Science, 322-6 Oroshi-cho, Toki 509-5292, Japan

E-mail contact of main author: toda@nifs.ac.jp

Abstract. The confinement property in helical toroidal plasmas is clarified. The analysis is performed by use of the one-dimensional transport equations with the effect of the radiative loss and the radial profile of the electric field. The analytical results in the edge region show the steep gradient in the electron temperature, which indicates the transport barrier formation. Because of the rapid increase of the radiative loss at the low electron temperature, the anomalous heat diffusivity is reduced near the edge. Next, the efficiency of the heating power input in the presence of the radiative loss is studied. The scaling of the critical density in helical devices is also derived.

1.   Introduction

The study of the plasma confinement physics is the urgent task of nuclear fusion research. The phenomena of the density limit control how the plasma performance is achievable. In tokamaks, the properties of the confinement and the density limit are dictated, e.g. [1]. The importance of the plasma dynamics and the critical density in the vicinity of the strong sources of impurities was discussed [2]. In helical plasmas, attention has been paid to the phenomena of the density limit, e.g. [3, 4]. The density limit phenomena in toroidal helical plasmas were examined with the analytic point model [5]. The helical plasmas have an additional freedom in magnetic geometry, which is utilized to investigate the transport mechanisms. Since the radial electric field determined by the ambipolar condition in a non-axisymmetric system is known to affect the confinement property, theoretical analysis of the density limit including the radiation loss in helical plasmas is necessary with the effect of the ambipolar radial electric field in a set of transport equations. The study of the density limit in helical plasmas is important specially in the case of an Internal Diffusion Barrier (IDB) [6] observed with a strong density gradient in a super dense core plasma in the Large Helical Device (LHD).

To examine the density limit for the thermal stability in helical plasmas, we add the term of the radiation loss rate of the energy to the temporal equation of the electron temperature in a set of one-dimensional transport equations. The radiative loss of the line emission from the impurity ions depends on the electron temperature as the loss increases if the electron temperature gets lower. The combined mechanism of the transport and the radiation loss of the energy is discussed. The dependence of the electron temperature profile on the electron heating is studied when the radiative loss is included in a set of the transport equations to examine the density limit in helical plasmas. The sharp decrease of the electron temperature is shown near the edge. This is because the radiative loss rate rapidly increases at the low electron temperature. The value of the anomalous heat diffusivity is significantly reduced near the edge. The characteristic of the transport barrier is shown. The efficiency ratio of the heating power input to the radiative loss is studied when we change the electron heating power. The parameter dependence of the critical density is derived, when the effect of the radial electric field is included.

2.   One-dimensional Model for Transport Equations

The one-dimensional transport model is employed. The cylindrical coordinate is used and r-axis is taken in the radial cylindrical plasma in this article. The region $0 \leq \rho \leq 1$ is considered, where a is the minor radius and $\rho = r/a$. For simplicity, the density profile from [6] is used for the Internal Diffusion Barrier (IDB) plasma as the temporally fixed density profile in the calculation here. This density profile is approximated as $n(\rho)_{\text{IDB}} = 4.62 \times 10^{20} + 2.89 \times 10^{20}\rho - 8.99 \times 10^{21}\rho^2 + 9.43 \times 10^{22}\rho^3 - 4.68 \times 10^{23}\rho^4 + 1.12 \times 10^{24}\rho^5 - 1.39 \times 10^{24}\rho^6 + 8.66 \times 10^{23}\rho^7\text{m}^{-3}$. The temporal equations for the electron temperature (T_e) and the hydrogen ion temperature (T_i) are analyzed in this article. The expression for the particle and heat neoclassical flux associated with helical-ripple trapped particles are given by the symbols Γ_j^{an} and Q_j^{an} for the species j, respectively. In the case of the calculation about the IDB with the high density plasma, we use the form for the radial neoclassical flux given in [7], which is available in the Pfirsch-Schlüter regime, because the plasma state of the IDB plasma corresponds to the high collisional regime. The total heat flux for the species j is given as $Q_j^{\text{t}} = Q_j^{\text{na}} - n\chi_a T_j' - 5D_a n' T_j/2$, where χ_a and D_a are the anomalous heat and particle diffusivities, respectively. In the calculation here, the convective energy flux term $-5D_a n' T_j/2$ in Q_j^{na} becomes the energy input flux except the energy heating source, because the energy input is necessary to compensate the particle loss when the density profile is temporally fixed. A theoretical model for the anomalous diffusivity is adopted. The equation for the electron temperature is given as

$$\frac{3}{2}\frac{\partial}{\partial t}(nT_e) = -\frac{1}{r}\frac{\partial}{\partial r}(rQ_e^{\text{t}}) - \frac{3m_e}{m_i}\frac{n}{\tau_e}(T_e - T_i) + p_{\text{he}} - p_z - p_b, \tag{1}$$

where the term τ_e denotes the electron collision time and the second term on the right hand side represents the heat exchange between ions and electrons. Here, the term p_z represents the radiative loss of the line emission from the impurity ions and the term p_b shows the bremsstrahlung loss. The form for p_z in the article [8] is used. The term p_{he} represents the absorbed power induced by the electron heating. The radial profiles of the electron heating term, p_{he} are assumed to be proportional to $\exp(-(r/(0.2a))^2)$ for the sake of the analytic insight. The temporal equation for the ion temperature is

$$\frac{3}{2}\frac{\partial}{\partial t}(nT_i) = -\frac{1}{r}\frac{\partial}{\partial r}(rQ_i^{\text{t}}) + \frac{3m_e}{m_i}\frac{n}{\tau_e}(T_e - T_i). \tag{2}$$

We use the ambipolar condition

$$\Gamma_i^{\text{an}} = \Gamma_e^{\text{an}} \tag{3}$$

with the hydrogen plasma to determine the radial profile of the electric field. The equations of the temperatures and electric field are solved coupled under the appropriate boundary conditions. We fix the boundary condition at the center of the plasma ($\rho = 0$) such that $T_e' = T_i' = E_r = 0$. The boundary conditions at the edge ($\rho = 1$), with respect to the temperature, are given by specifying the gradient scale lengths. We employ those expected in LHD: $-T_e'/T_e = -T_i'/T_i = 0.01\text{m}$ in this article. The machine parameters which are similar to those of LHD are set to be $R = 3.6\text{m}$, $a = 0.6\text{m}$, $B = 3\text{T}$, $\ell = 2$ and $m = 10$. In this article, we set the safety factor and the helical ripple coefficient as $q = 1/(0.4 + 1.2\rho^2)$ and $\epsilon_h = 2\sqrt{1 - (2/(mq(0)) - 1)^2}I_2(mr/R)$, respectively. Here, $q(0)$ is the value of the safety factor at $\rho = 0$ and I_2 is the second-order modified Bessel function.

3. Model of Anomalous Transport Coefficients

We adopt the model for the anomalous heat diffusivity χ_a based on the theory of the self-sustained turbulence due to the interchange mode [9] and the ballooning mode [10], both driven by the current diffusivity. The anomalous transport coefficient for the temperatures is given as $\chi_a = \chi_0/(1 + G\omega_{E1}^2)$ $(\chi_0 = F(s, \alpha)\alpha^{3/2}c^2 v_A/(\omega_{pe}^2 qR))$, where ω_{pe} is the electron plasma frequency. The factor $F(s, \alpha)$ is the function of the magnetic shear s and the normalized pressure gradient α. The parameter ω_{E1} represents the effect of the reduction of the anomalous transport due to the shearing rate of the radial electric field. The details about the parameters F and G were given in [9, 10]. The value for the anomalous diffusivities of the particle is set as $D_a = \chi_a$. We have studied the establishment of the electron Internal Transport Barrier (e-ITB) by the E_r transition in helical device [11], when we use this model for the anomalous heat diffusivity.

4. Results of the Analysis

4.1 Classification by the Ratio of the Radiative loss

To examine the density limit for the thermal stability in the case of the IDB, we add the term of the radiation loss rate of the energy to the temporal equation of the electron temperature. The combined mechanism of the transport and the radiation loss of the energy is discussed. The form of the radiative loss rate was given in [8]. We classify the calculation results into the three states by the ratio of the radiative loss: (i) When the heating power is high, the transport loss is dominant compared with the radiative loss. (ii) When the heating power decreases, the radiative loss becomes substantial and we have the partially-detached state in the electron temperature profile. (iii) When the heating power decreases further, the radiative loss becomes dominant compared with the transport loss. The fully-detached state characteristic is obtained in the profile of the electron temperature. The profile of the radiative loss can be obtained as a temporally stable one in the wide region of the electron heating power.

4.2 Radial Structure of the Radiative Loss

We take an oxygen plasma with $n_{oxygen} = 0.01n$, where n_{oxygen} is the density of the oxygen. For simplicity, the density profile from [6] is used for the IDB plasma as the temporally fixed density profile in the calculation here. This density profile is temporally fixed as a radial profile shown in section 2. We examine the temporal evolutions of the electron and ion temperatures, and the profile of the radial electric field from the ambipolar condition. The strong dependence of the radiative loss on the electron temperature significantly changes the plasma state. An example of the results is shown below. Stationary plasma profiles are obtained with electron heating power values of 6.7 MW (solid lines) and 12 MW (dashed lines) for $0.8 < \rho < 1.0$ in figure 1. Figure 1(a) shows the radial profiles of the radiative loss p_z in the region $0.8 < \rho < 1.0$. The radiative loss has a strong peak at low temperature near $\rho \simeq 0.935$ and shows the fully-detached plasma state in the case of 6.7MW. The radiative loss strongly increases near $\rho \simeq 1.0$ and show the partially-detached state in the case of 12MW. The case of 6.7MW corresponds to the state (iii) and the case of 12MW corresponds to the state (ii) in the previous subsection, respectively. We obtain the temporally stable profiles of the radiative loss in the cases of 6.7MW and 12MW. The radiative loss rate takes
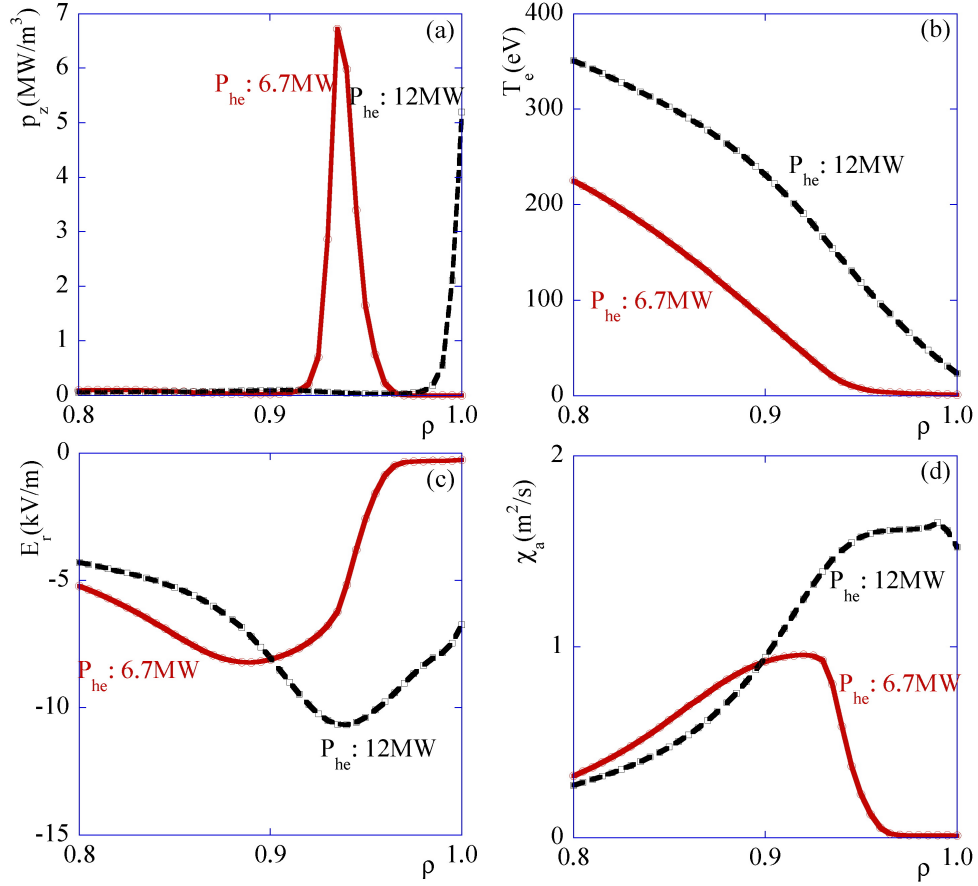
FIG. 1 Radial profiles in the region $0.8 < \rho < 1.0$ for the electron heating power of 6.7MW (solid lines) and 12MW (dashed lines). (a) The radiative cooling rate. (b) The electron temperature with the effect of the radiative loss. (c) The radial electric field. (d) The anomalous heat diffusivity χ_a.

a peak at around $T_e = 20$eV and has about a half value at around $T_e = 10$eV and $T_e = 30$eV, compared with the value at $T_e = 20$eV. The profiles of the electron temperature are also shown in figure 1(b) with two cases of the electron heating in the region $0.8 < \rho < 1.0$. In the case that the electron heating is 6.7MW, the sharp decrease of the electron temperature is shown and the rapid change of the electron temperature gradient is obtained, because there is a strong peak in the radial profile of p_z at $\rho = 0.935$. The characteristic of the transport barrier is studied. In the case that the electron heating is 12MW, the strong change of the electron temperature gradient is not obtained. It is found that the strong increase of p_z at $\rho = 1.0$ is not enough to realize the transport barrier. The radial profiles of the ambipolar radial electric field are shown in two cases the electron heating are 6.7MW and 12MW in the region $0.8 < \rho < 1.0$ in figure 1(c). The radial electric field takes a large negative value in the region $\rho < 0.935$ in figure 1(c) because of the steep temperature gradient in the case of 6.7MW. In the region $\rho > 0.935$, the value of E_r radially changes to the value which is close to zero near the edge because of the weak gradient of the temperature, when the radial electric field is determined by the ambipolar condition here. The phenomena like the transition at $\rho = 0.935$ in the E_r profile is obtained only in the case that the electron heating power

is 6.7MW. The value of the anomalous heat diffusivity is significantly reduced in figure 1(d) due to the change of the electron temperature gradient near the edge in figure 1(b), when the electron heating power is 6.7MW. This is because the model of the anomalous heat diffusivity used here has the dependence on the pressure gradient as $\chi_a \propto \alpha^{3/2}$. This reduction of χ_a depends on the choice of the model for the anomalous heat diffusivity. The shear of the radial electric field is not enough to suppress the anomalous heat diffusivity in the edge region. If we set $G = 0$ and neglect the effect of the radial electric field shear in the form of the anomalous heat diffusivity χ_a, the main point in this article that the transport characteristic is shown does not alter. In the core region ($\rho \sim 0.2$), the reduction of the anomalous heat diffusivity is obtained due to the shear of the radial electric field in the parameter region examined here. Therefore, the profile of the radial electric field affects the confinement property. In the case of 12MW, no rapid reduction of the anomalous heat diffusivity is shown in figure 1(d) because there is no large change of the electron temperature gradient near the edge. The transport characteristic is studied in the edge region $0.8 < \rho < 1.0$ from the rapid increase of the radiative loss at the low electron temperature ($10\text{eV} < T_e < 30\text{eV}$).

4.3   Access to the Fully-Detached Stable State

We discuss the dependence of the sum of the radiative loss and bremsstrahlung loss on the density divided by the effective power. If the effective power decreases, we consider the situation that the "effective" density increases. The effective power means the sum of the contribution from the convective term, the heat exchange and the heating power in the temporal equation of the electron temperature (1), because the energy input is needed to compensate the particle loss when the density profile is temporally fixed. Here, we use the quantity P_z, P_b and P_{eff} related with the radiative loss, the bremsstrahlung loss and the effective power input, which are integrated in the toroidal coordinate and the approximation $r/R = 0$ is used. In figure 2(a), the dependence of the sum of the radiative loss and bremsstrahlung loss on the line-averaged density divided by the effective power is shown. In the enclosed region of figure 2(a) labeled by parameter region (A), the heating power is around 10MW. The heat exchange term plays a role of the power loss in the region (A), because the electron temperature is higher than the ion temperature at all radial points. In this region (A), the effective input power is lost by the radiative loss and bremsstrahlung loss with the ratio 65%. We have the contribution from the conductive term in equation (1) , because the electron temperature gradient at $\rho = 1$ has some value in the region (A). Therefore, we have a loss by around 35% of the conductive loss due to the electron temperature gradient at $\rho = 1$, compared with the effective input power in the parameter region (A). The power input which comes from the convective term in the equation (1) is negligible in the parameter region (A). In this region (A), the partially-detached plasma state is obtained. Therefore, the region (A) corresponds to the state (ii) in the subsection 4.1. Next, we consider the case that the heating power is around 7MW in the enclosed region of figure 2(a) labeled by parameter region (B). The heat exchange term plays a role of the power input in the region (B), because the ion temperature is slightly higher than the electron temperature at certain radial points. In this parameter region, the effective input power is almost lost by the radiative loss and bremsstrahlung loss with the ratio $(P_z + P_b)/P_{\text{eff}} \sim 1$. We have no contribution in the integrated quantity from the conductive term in equation (1), because the electron temperature gradient at $\rho = 0$ is zero and T'_e at $\rho = 1$ is close to zero in the region (B). In this region (B), we have the fully-detached plasma state. Therefore, the region (B) corresponds to the state (iii) in the subsection 4.1. We obtain the fully-detached and partially-detached plasma
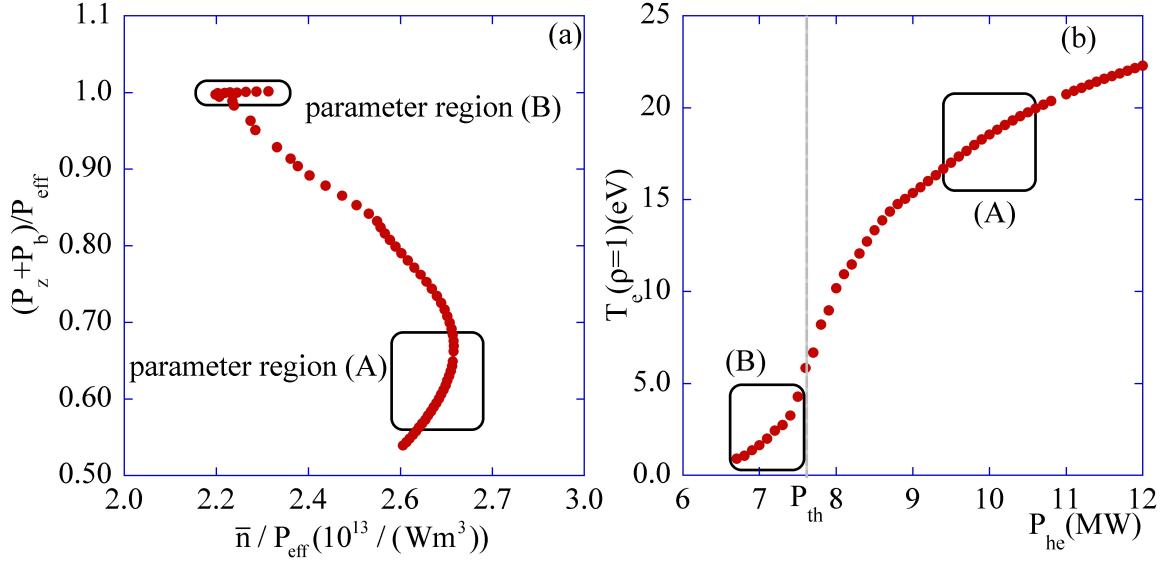
FIG. 2 (a) The dependence of the sum of the radiative power and the bremsstrahlung loss on the line-averaged density divided by the effective input power. (b) The electron temperature at $\rho = 1$ depending on the electron heating power.

states which is temporally stable in the wide region of the electron heating input.

Figure 2(b) shows the dependence of the electron temperature at $\rho = 1$ on the electron heating power P_{he}. The labeled regions by (A) and (B) in figure 2(b) corresponds to the regions labeled by 'parameter region (A)' and 'parameter region (B)' in figure 2(a), respectively. The radiative loss rapidly increases at the low electron temperature ($10eV < T_e < 30eV$). The threshold heating power is estimated as $P_{th} \simeq 7.6MW$ for the boundary between the partial-detached and the fully-detached plasma states. In the region $P_{he} \geq 7.6MW$, the relation is approximatedly obtained as $T_e - T_e(P_{th}) \propto (P_{he} - P_{th})^{0.34 \pm 0.02}$. When the heating power P_{he} is less than P_{th}, the dependence of the electron temperature on the heating power P_{he} gets weak. Therefore, even in the case of the low heating power ($P_{he} \leq 6.5MW$), the fully-detached plasma state is found to be achievable.

4.4   Density Limit

We determined the threshold heating power P_{th} for the boundary between the fully-detached and the partially-detached stable plasmas in the previous subsection, when the radiative loss and the transport loss are included using a set of temporal transport equations of the temperatures of electrons and ions and the ambipolar radial electric field. We use temporally fixed density profiles, where $n(\rho) = \gamma n(\rho)_{IDB}$ and the parameter γ is chosen to take the value $0.6 \leq \gamma \leq 1.2$ in this calculation. The threshold electron heating power P_{th} is the function of the line-averaged critical density $\bar{n}_c$. The condition $P_e \geq P_{th}$, can be shown as $\bar{n} \leq \bar{n}_c$, where P_e is the electron heating power. The dependence of the critical density $\bar{n}_c$ on the threshold electron heating power P_{th} is given in figure 3. The solid line in figure 3 shows the critical density $\bar{n}_c$ as the function of P_{th}, $\bar{n}_c \propto P_{th}^{0.65 \pm 0.01}$. The Sudo scaling of the density limit was shown from the experimental results in helical plasmas as $n_{Sudo} \propto P^{0.5}$, where P is the absorbed power [3]. The dependence of the critical density on the

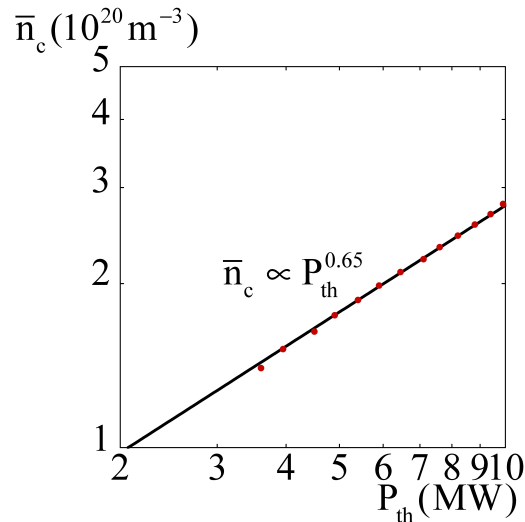$$\bar{n}_c (10^{20}\,\mathrm{m}^{-3})$$

FIG. 3 The dependence of the line-averaged critical density $\bar{n}_c$ on the threshold electron heating power P_{th} in the logarithmic scales on both the horizontal and vertical axes. The solid line approximately follows the relation $\bar{n}_c \propto P_{th}^{0.65}$.

threshold electron heating power derived in the case of the IDB here is slightly stronger than the case of the Sudo scaling of the density limit. If we neglect the effect of E_r' (set $G = 0$), we obtain the close relation for the critical density to the case with the effect of the E_r gradient for the choice of χ_a in this article. This is because the mechanism of the radiative loss in the edge region mainly determines the dependence of the critical density on the electron heating power for the density limit.

5. Summary

The analysis is performed by use of the one-dimensional transport equations with the effect of the radiative loss and the radial profile of the ambipolar electric field. The dependence of the electron temperature on the electron heating was studied in the case of the IDB plasma with the radiative cooling rate. The strong peak of the radiative loss is shown near the edge at the low electron temperature. The analytical results in the edge region show the steep gradient in the profile of the electron temperature, which indicates the characteristic of the transport barrier formation. The ratio of the radiative and bremsstrahlung loss to the effective input power is examined when we calculate the different cases of the electron heating power. The fully-detached and partially-detached plasma states which are temporally stable are obtained in the wide parameter region. The parameter dependence of the critical density on the electron heating power is shown. The large improvement in the density limit scaling is not found due to the effect of the E_r gradient. The parameter dependence of the critical density changes because of the impurity species and needs to be compared with the experimental results in detail. The dependence of the critical density on the profile of the electron heating should be also studied. These are left for future studies.

References

[1] GREENWALD, M. et al., "New look at density limits in tokamaks", Nucl. Fusion **28** (1988) 2199.

[2] TOKAR, M. Z., et al., "Modeling of detachment in a limiter tokamak as a nonlinear phenomenon caused by impurity radiation, Plasma Phys. Control. Fusion **36** (1995) A241.

[3] SUDO, S., et al., "Scalings of energy confinement and density limit in stellarator/heliotron devices", Nucl. Fusion **30** (1990) 11.

[4] WAGNER, F., et al., "H-mode of W7-AS stellarator", Plasma Phys. Control. Fusion **36** (1994) A61.

[5] ITOH, K., et al., "Modelling of density limit phenomena in toroidal helical plasmas", J. Phys. Soc. Jpn **70** (2001) 3274.

[6] OHYABU, N., et al., "Observation of stable super dense core plasmas in the Large Helical Device", Phys. Rev. Lett. **97** (2006) 055002.

[7] SHAING, K. C. and CALLEN J. D., "Neoclassical flows and transport in nonaxisymmetric toroidal plasmas", Phys. Fluids **26** (1983) 3315.

[8] POST, D. E. and JENSEN, R. V., "Steady-state radiative cooling rates for low-density, high-temperature plasmas", Atomic Data and Nuclear Data Tables **20** (1977) 397.

[9] ITOH, K., et al., "Confinement improvement in H-mode-like plasmas in helical systems ", Plasma Phys. Control. Fusion **36** (1994) 123.

[10] ITOH, K., et al., "Self-sustained turbulence and L-mode confinement in toroidal plasmas I ", Plasma Phys. Control. Fusion **36** (1994) 279.

[11] TODA, S., et al.,"Transport analysis of the effect of zonal flows on the electron internal transport barriers in toroidal helical plasmas", Nucl. Fusion **47** (2007) 914.